
Boosting Local Causal Discovery in High-Dimensional Expression Data

Philip Versteeg

University of Amsterdam
Amsterdam, the Netherlands
p.j.j.p.versteeg@uva.nl

Joris M. Mooij

University of Amsterdam
Amsterdam, the Netherlands
j.m.mooij@uva.nl

Abstract

We study how well Local Causal Discovery (LCD) [Cooper, 1997], a simple and efficient constraint-based method for causal discovery, is able to predict causal effects in large-scale gene expression data. We construct practical estimators specific to the high-dimensional regime. Inspired by ICP [Peters et al., 2016], we use an optional preselection method and two different statistical tests. Empirically, the resulting LCD estimator is seen to closely approach the accuracy of ICP, the state-of-the-art method, while it is algorithmically simpler and computationally more efficient.

1 Introduction

One of the main goals of empiricism is uncovering relationships that underly the data at hand. Scientific question often aim for the estimation of causal quantities instead of statistical associations. Causal models can predict perturbations (interventions) to the system, allowing one to reason about previously unseen experiments that are too costly, difficult or unethical to perform.

One approach to causal inference is constraint-based, where statistical evidence in the data on multiple variables at a time is combined to limit the space of possible causal effects. The PC and FCI algorithm [Spirtes et al., 2000] use independence testing under certain assumptions to ingeniously infer a set of possible causal graphs. These methods are sound and complete under their respective assumptions, but require a (possibly very slow) global search when the variable set is large and relations are non-sparse. Furthermore, they are traditionally only applied to observational data, not making use of any perturbation data that may be available.

The LCD algorithm [Cooper, 1997], one of the simplest constraint-based causal discovery methods, uses background information that can be derived from experiments and (in)dependence relations to make a single cause effect prediction for subsets of three variables locally. The algorithm is algorithmically generic and many practical estimators are possible. Specifically, a conservative estimator of LCD has been used to infer protein signaling networks from mass cytometry data [Triantafillou et al., 2017]. Another LCD estimator is Trigger [Chen et al., 2007].

The more recently introduced ICP algorithm [Peters et al., 2016] requires data from multiple contexts. Under certain assumptions, it can be shown to predict causal effects by exploiting conditional distributions that are invariant under changes of the context. In Meinshausen et al. [2016], ICP predictions are assessed with real-world expression data [Kemmeren et al., 2014], and results are shown to be significant when compared to an internal data-driven ground-truth and several externally sourced gold-standards.

We focus on the statistical aspects of LCD and apply it to predict knock-out effects in large-scale gene expression data [Kemmeren et al., 2014]. Inspired by the implementation of the ICP estimator, we construct several practical versions of LCD that are well-suited to this high-dimensional task. In

particular, we apply L_2 -boosting, a fast gradient boosting regression method for variable selection in the high-dimension setting [Bühlmann and Yu, 2003], to limit the search space of LCD. We also examine the effect of using different statistical tests in the LCD estimator.

The experiments are performed on train-test splits of gene expression data [Kemmeren et al., 2014] containing “pure observations” and knock-outs. Here one part of the knock-out data serves as the background information that can be used in prediction methods, while the remaining data are used to construct a ground-truth set. We compare the performance of the LCD estimators to ICP, the state-of-the-art method for this dataset [Meinshausen et al., 2016] that exploits the perturbed data in a more sophisticated approach. We find that implementing the preselection procedure with LCD results in cause effect predictions that evaluate comparably to ICP, while LCD is computationally more efficient. The choice of the statistical test was not seen to affect results.

We start by concisely introducing causal models and causal inference from both observational and interventional data. Then we discuss the main methods in this work, LCD and ICP, and their estimators. We outline the experimental approach and provide results for experiments on gene expression data, before we close with conclusions.

2 Preliminaries

Here we shortly introduce causal graphs and methods for causal inference from observational and interventional data.

2.1 Graphical Causal Models

We consider a set of p random variables \mathbf{X} , for which the observed causal relationships are modeled as edges between nodes (variables) in a directed graph (DG). Here, a directed edge $X \rightarrow Y$ between $X, Y \in \mathbf{X}$ corresponds to a *direct causal effect* relative to \mathbf{X} . An *ancestral causal effect*, typically plainly referred to as a *causal effect*, then corresponds to the existence of a sequence of direct causal effects $X \rightarrow W \rightarrow V \rightarrow \dots \rightarrow Y$. The set of direct causes of a target variable Y is denoted as its *parents* (or $\text{pa}(Y)$), while the set of its ancestral causes is referred to as its *ancestors* (or $\text{anc}(Y)$). When unmeasured confounding is present (in the case without *causal sufficiency*), the causal graph is a directed mixed graph (DMG) that contains bidirected edges between variables, indicating latent unmeasured variables.

A common way of modeling observational and interventional data related to a causal graph is with a Structural Causal Model (SCM) [Pearl, 2009].¹ In essence, an SCM specifies a single equation for each *endogenous* variable X_i ,

$$X_i = f_i(\text{pa}(X_i), N_i), \quad (1)$$

where f_i is a function of the parent set $\text{pa}(Y)$ and an *exogenous* noise variable N_i . The solutions of these structural equations, together with the distributions of the exogenous noise terms, specify the joint observational distribution $\mathbb{P}(\mathbf{X})$. Perfect interventions are modeled by replacing the right-hand side of (1) for all targeted variables $i \in \mathbf{I} \subseteq \mathbf{X}$ by the corresponding fixed value ξ_i , inducing the corresponding *interventional distribution* $\mathbb{P}(\mathbf{X} \mid \text{do}(\mathbf{X}_{\mathbf{I}} = \boldsymbol{\xi}_{\mathbf{I}}))$. We refer the reader to Pearl [2009] and Bongers et al. [2016] for a detailed treatment on SCMs.

2.2 Constraint-based Causal Discovery

The *Markov assumption* (see e.g. Pearl [2009] and Forré and Mooij [2017] for an overview) relates statistical properties of a causal graph to independence constraints in observed data. Missing edges in the causal graph imply (conditional) independences of the form $X \perp\!\!\!\perp Y \mid \mathbf{Z}$, for $\mathbf{Z} \subset \mathbf{X}$, through the d -separation criterion (see e.g. [Spirtes et al., 2000, Pearl, 2009]) in the acyclic case.² Under the

¹Technically we consider the class of Simple SCMs here (see Mooij et al. [2016]), for which, relative to a given SCM, the formal probabilistic definitions of (direct) causal effects coincide with the more informal notations here.

²Recent advances have non-trivially extended d -separation to cyclic models by introducing σ -separation [Forré and Mooij, 2017]. It can be shown that the LCD and ICP (reformulated in JCI-1 terms) methods are valid when cycles are present for Simple SCMs by using this separation criterion under certain modeling assumptions [Mooij et al., 2016]. As it is not the main focus of this work, we will treat methods mainly in terms of acyclic models and d -separation.

faithfulness assumption the reverse implication holds, such that *all* independences present in the data correspond to pairs of separated variables.

Algorithms in a class of *constraint-based* causal discovery methods build on this principle, learning (direct) causal effects from independence statements that are derived from observational data. The PC algorithm combines independences between all pairs of variables in a clever search to recover (as much of) an acyclic causal graph under causal sufficiency, whereas the FCI algorithm extends this strategy to cases where confounding and selection bias are present [Spirtes et al., 2000]. These methods can be computationally prohibitive for systems with a large number of variables, as the search can require a large number of pairwise tests. Local strategies such as Y-Structures [Mooij and Cremers] and LCD [Cooper, 1997] (see Sec. 3.2) trade off completeness for the ability to scale to a large number of variables.

2.3 Interventional Data and JCI

In almost all practical situations, only a subset of the causal effects is recoverable from independence statements derived from purely observational data. Even in the infinite sample limit, observational constraint-based causal discovery is in general feasible up to an equivalence class that represents multiple indistinguishable graphs. The identifiability of causal effects can be increased by the inclusion of interventional samples.

The recently introduced Joint Causal Inference (JCI) [Mooij et al., 2016] is a framework for incorporating various types of experimental data jointly in causal learning problems. Perfect interventions (and other manipulations) are jointly modeled through multiple *context variables*, in addition to the regular endogenous *system variables*, and a set of underlying assumptions. For example, samples from multiple datasets can be combined by including a single context variable to the dataset, resulting in an extra integer column in the dataset that encodes the originating dataset of each sample. The main idea of JCI is to then jointly learn over the meta-system of combined system and context variables, while encoding a set of required assumptions on context variables as background knowledge.

The JCI assumptions that are relevant for methods in this work are given as follows, where \mathcal{C} and \mathbf{X} now denote sets of context and system variables respectively.

Assumption 0 (Joint SCM) *The data-generating process underlying \mathcal{C} and \mathbf{X} is modeled by a single SCM.*

Assumption 1 (Exogeneity) *No system variable $X \in \mathbf{X}$ is an ancestor of any context variable $C \in \mathcal{C}$.*

This combined modeling assumption is labeled as the JCI-1. We refer the reader to Mooij et al. [2016] for additional JCI assumptions related to context models that are outside the scope of this work.

As a simple example of a JCI-1 model, consider the Randomized Controlled Trial (RCT), where the causal effect of a randomized treatment on a single outcome variable Y is studied. Here the context C indicates the treated population ($C = 1$) and the control group ($C = 0$), expressing the belief that outcome of the treatment does not effect the treatment itself. Under these conditions, i.e. assuming JCI-1, and when there is no confounding and selection bias, then a statistical dependence between C and Y implies a causal effect of C on Y .

3 Methods

We first describe the two causal prediction methods that are central to this work in the terminology of JCI. We discuss practical estimators for each algorithm specifically.

3.1 Invariant Causal Prediction

The Invariant Causal Prediction (ICP) [Peters et al., 2016] algorithm predicts a conservative subset of the true parent set for a given target variable Y by identifying conditional distributions that remain invariant under changes of a single context variable C , also referred to as the *environment*. In the original formulation, ICP assumes that there is no causal effect from C to Y in addition to causal

sufficiency and acyclicity, but it remarkably does not require the faithfulness assumption. One of the main statistical aspects is its ability to set a confidence level for which subsets are accepted.

In Mooij et al. [2016] it is shown that ICP can be reformulated in terms of JCI-1 when faithfulness is additionally assumed, and the interpretation proposed there also allows for cycles to be present. ICP then outputs a subset of the true ancestors of Y instead of a subset of the parent set.

We now describe several statistical aspects of a practical ICP estimator, which is one of possible choices given the generic ICP algorithm.

Statistical Test The original ICP variant [Peters et al., 2016] tests at confidence level α if a linear SCM exhibits invariant model parameters across realizations c of C for a given target effect Y . The authors of Peters et al. [2016] propose two practical estimators, a regression based test and an approximate test. For the first we refer to Sec. 3.1.1 in Peters et al. [2016], while the second test, which we label a *mean-variance* test, is constructed as follows.

For each potential parent set, i.e. each subset of $\mathbf{X} \setminus \{Y\}$, and each context $c \in C$, the mean of the residuals of a linear regression in c is compared to the mean of the residuals in all others contexts $C \setminus \{c\}$ with a t -test. The resulting p -values are combined across contexts with a Bonferroni correction. Analogously, an F -test for the variances of the residuals is performed across contexts and combined in the same way. The p -value of the potential parent set is the minimal of the two values, and the final parent set is chosen as the intersection of all potential parents the are not rejected at level α .

Preselection In the worst case, ICP scales exponentially in the number of system variables p by examining all subsets of variables as potential causes. To circumvent this problem, [Peters et al., 2016] suggests a priori limiting the set of potential causes for each target Y through a preselection method. Their proposal is to take a number of top ranking non-zero coefficients from a Lasso [Tibshirani, 1996] or L_2 -boosting [Schapire et al., 1998] regression.

ICP Estimator For each of the above options, we pick the default in the `InvariantCausalPrediction` R package for the high-dimensional setting encountered here. This practical ICP estimator uses the mean-variance test and the L_2 -boosting preselection.³

3.2 Local Causal Discovery

Local Causal Discovery (LCD) [Cooper, 1997] is a constraint-based causal discovery method, combining three (in)dependence tests with causal background knowledge. It requires that the data includes (at least) one context variable C subject to JCI-1 assumptions and that selection bias is not present in the samples. LCD does not assume causal sufficiency and cycles may be present in the modern formulation [Mooij et al., 2016].

LCD tests if the following constraints hold for a given triplet of variables (C, X, Y) :

$$\begin{aligned} C &\perp\!\!\!\perp Y|X \\ C &\not\perp\!\!\!\perp X \\ X &\not\perp\!\!\!\perp Y \end{aligned} \tag{2}$$

where $X, Y \in \mathbf{X}$ and $\not\perp\!\!\!\perp$ denotes statistical dependence. It then follows that X is a direct cause of Y relative to $\{C, X, Y\}$, Y is not a direct cause of X and that no confounding is present between X and Y . One straightforward proof is to enumerate all possible DMGs for three variables where these (in)dependences and the JCI-1 assumption holds, resulting in the three DMGs in Fig. 1.

As the LCD result holds under confounding, it can straightforwardly be applied to systems with more than three variables by iterating over (all) subsets of triples, each time marginalizing out all other variables. The LCD prediction is then an *ancestral* causal effect, rather than a *direct* causal effect, relative to all system and context variables.

Compared to ICP, the LCD algorithm exhibits less power in predicting causal effects. ICP predicts the causal effect $X \in \text{pa}(Y)$ in each of the LCD patterns in Fig. 1, but it can additionally infer

³We use small capitalization to label estimators.

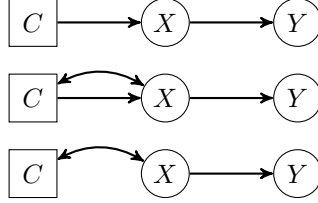


Figure 1: All three variable DMGs with context C where LCD predicts that $X \in \text{pa}(Y)$ relative to $\{C, X, Y\}$.

multiple parents for a single effect when configured as in Fig. 2. The latter pattern is omitted by LCD, as marginalizing over X_1 (or X_2) leads to a dependency between C and Y even when conditioning on X_2 (or X_1). Note however that ICP is less efficient, as it potentially searches over all possible subsets of $\text{pa}(Y)$, whereas LCD has a computational complexity of $\mathcal{O}(p^3)$.

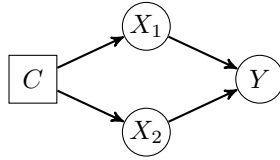


Figure 2: Example of a DMG with context C where LCD does not make a prediction, but where ICP returns $\{X_1, X_2\}$ as parent set of Y .

We introduce four practical LCD estimators here that each implement the generic LCD algorithm described above. Each one of these estimators is a combination of the following options.

Statistical Test We consider two options for testing the (in)dependences in (2) at confidence level α . Following common practice in constraint-based literature, we accept independence whenever $p \geq \alpha$.

We can use the same combined mean-variance test as used by the ICP estimator in Sec. 3.1 to find potential parent sets.

Alternatively, we use a (partial)correlation test, one of the simplest (conditional) independence test that is used extensively in constraint-based causal discovery. The p -value for the null hypothesis of independence is computed using the Student's t transform of the (partial) correlation coefficient.

Preselection As LCD scales reasonably well with the number of variables p , it is generally possible to compute all possible LCD triples for large p with a fast test.

Alternatively, we use L_2 -boosting as a preselection method inspired by the ICP estimator. Then we only test for LCD triples (C, X, Y) if X is found in the variable selection for Y for suitable tuning of the boosting method.

LCD Estimators This results in the following practical LCD estimators.

- LCD: no preselection and the partial correlation test.
- LCD-MV: no preselection and the mean-variance test.
- LCD-BST: L_2 boosting as preselection and the partial correlation test.
- LCD-BST-MV: L_2 boosting as preselection and the mean-variance test.

3.3 Boosting Baseline

An interesting non-causal baseline is simply obtained by computing the L_2 -boosting preselection method for each target variable Y and naively labeling the set of selected variables (that are predictive for Y) as the causes of Y .

4 Experiments

We apply LCD and ICP estimators on train-test splits of gene expression data that contains both observations and interventional samples. We define a target ground-truth score, derived from the “true” interventional measurement and observational samples, and assess the performance of each predictor against this score.

4.1 Experimental Setup

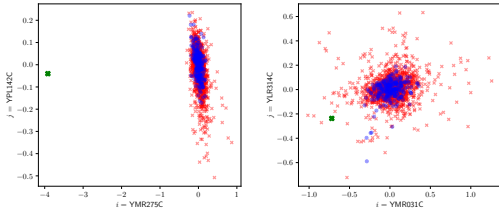


Figure 3: Examples of pairwise gene expressions (i, j) from the Kemmeren et al. [2014] dataset. Observational and interventional samples are shown in blue and red, while the knock-out of the gene i , which expression is displayed on the horizontal axes (e.g. $YMR275C$ and $YMR031C$), is indicated by the green cross.

Data

We use data from microarray experiments from Kemmeren et al. [2014], where, after preprocessing, 262 *observational* samples are available for each of 6170 genes.⁴ Additionally, in 1479 knock-out experiments a unique single gene has been externally disabled (intervened) and the expression level is measured once for all 6170 genes. In Fig. 3 we show how these *interventional* samples differ from observational data for a few example gene pairs.

Train-Test Split

In a train-test setup, we split the dataset in five disjoint partitions, each part containing 1/5th of the observational samples and 1/5th of the interventional experiments. Each of these parts is used as a test set once, where the knock-out data are used to construct the “true” causal effect of interventions disjoint from the training set. The remaining four parts are combined as a training set, which therefore contains all interventional samples that are *not* the target “true” causal effect, but which can be used for training. The training data are prepared as a joint JCI dataset with a single context variable and 6170 system variables, where all observations are gathered in $C = 0$ and all interventions in $C = 1$.

Ground-Truth Definition

The interventional samples, where a single knock-out has been performed, straightforwardly relate to the existence of (ancestral) causal effects. A difference in the interventional distribution $\mathbb{P}(Y|\text{do}(X))$ from the observational distribution $\mathbb{P}(Y)$ implies that $X \in \text{an}(Y)$, where all other variables $\mathbf{X} \setminus \{X, Y\}$ are marginalized [Peters et al., 2017]. This allows us to construct a ground-truth score from the interventional data that scores causal effect as follows.

Let the expression of gene j measured under intervention i be denoted as $X_{j;i}$. This single interventional sample represents the raw expression level in the units of measure of gene j , independent of its natural observational state. We standardize it with respect to the observational expression levels of this gene, resulting in the following score:

$$S_{ij}^{\text{std}} = \frac{|X_{j;i} - \mu_j|}{\sigma_j}, \tag{3}$$

⁴Original and preprocessed data files are available at http://deleteome.holstegelab.nl/downloads_causal_inference.php.

where σ_j and μ_j give the empirical mean and standard deviation of the expression level of gene j in the observational data. We compute this score for all interventions and all genes that are available in each test set and merge the score afterwards over all pairs. The result is a total of 9119260 scored ground-truth pairs, where we have excluded self-effects.

Evaluation

For a given training set, predictions for each causal method are computed only for those intervention-gene pairs (i, j) for which the intervention is available in the respective test set. The total prediction score is merged afterwards over all partitions. The continuous ground truth score S_{ij}^{std} is thresholded at a desired prevalence level to produce a ground-truth set of “true” pairs. The pairs which rank highest by each of the prediction methods are then compared with this set in a ROC curve, where the recall, or true positive rate (TPR), is set out against the sensitivity, or false positive rate (FPR).

4.2 Method Implementation

We used the `InvariantCausalPrediction` [Peters et al., 2016] R package to compute ICP predictions (Sec. 3.1). We closely follow the approach of Meinshausen et al. [2016]: the confidence level for the ICP estimator is set at 0.01 and `stopIfEmpty` is set to `TRUE` for faster computation, while all other settings are left to the defaults. This implies that L_2 -boosting is used as preselection method, which calls the `glmboost` routine from the `MBoost` R package. Here the tuning parameter is set at the ICP default, such that a maximum of 8 variables are selected as potential parents for each target variable, while all other parameters are left at default options. Note that this variable selection is also computed over the joint data, which includes all observational and interventional samples.

For the LCD estimators (Sec. 3.2) we use the same settings as ICP whenever applicable: a confidence level of 0.01 for each of the statistical tests is used, and the same construction of the L_2 -boosting is applied in for preselection in LCD-BST and LCD-BST-MV.

The non-causal L_2 -boosting baseline (Sec. 3.3) uses the same preselection construction as described above for LCD and ICP.

All prediction methods are trained over 100 random subsamples of the training data to increase the stability of predictions in the high-dimensional setup [Bühlmann and van de Geer, 2011]. In the subsampling procedure, the joint observational and interventional data are sampled uniformly at a fraction of 0.5 without replacement. The resulting final stable [Meinshausen and Bühlmann, 2010] estimator for each prediction method is then given as the number of pairs predicted across all subsamples.

Lastly we attempted to compare with the Trigger estimator [Chen et al., 2007], which assumes that a natural (Mendelian) randomization of the genetic information underlies the data and then combines a sequence of likelihood ratio tests. We found however that the practical estimator in the `Trigger` R package could not be successfully on a pooling of the knock-out expression data with context variables.

4.3 Results

The results of the experiments are shown in Fig. 4, where the ICP, LCD and the baseline estimators are compared to the top scoring pairs according to the ground-truth score (3). ROC curves are shown at three different levels of prevalence, where in each figure we vary the number of true effects that are in the ground-truth set.

Surprisingly, the L_2 -boosting baseline shows a very effective selection of the first few hundred pairs in the ground-truth set. Nonetheless, it is still outperformed by the addition of the ICP and LCD methods for the top pairs, as expected.

We find that ICP outperforms other methods for this definition of the ground-truth, where a large portion of the highest scoring predictions (i.e. the pairs that are predicted most frequently across all random subsamples) matches with the top 10%, 1% and 0.1% pairs in the ground-truth. This reaffirms the findings of Meinshausen et al. [2016], where a different ground-truth definition is used.

The simplest LCD-type estimator, LCD, shows better-than-random results at the 10% prevalence, but this is reduced to random guessing levels for the harder prediction tasks at lower prevalences. The

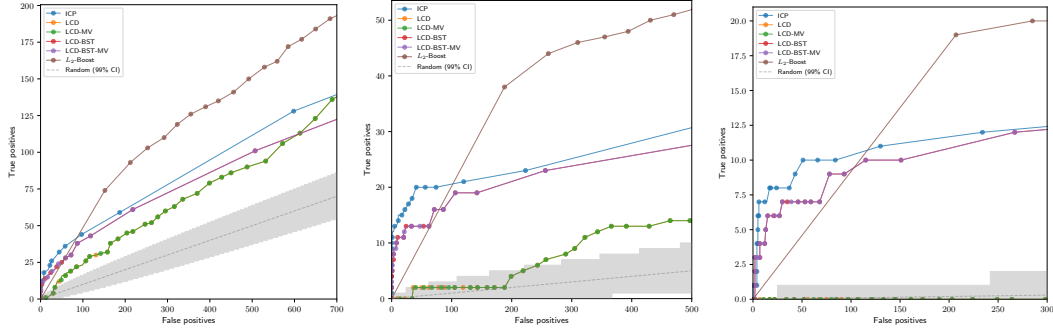


Figure 4: ROC curves for the top predictions of ICP, four LCD estimators and the L_2 -boosting baseline in a 5-fold train-test split of the gene expression data. Curves for LCD almost completely match LCD-MV, and similarly for LCD-BST and LCD-BST-MV. From left to right, the ground-truth is composed of the 10%, 1% and 0.1% of the top scoring pairs according to S_{ij}^{std} respectively. Random guessing with a 99% confidence interval is shown in gray.

same applies to LCD-MV, which uses the mean-variance test. Applying a L_2 -boosting preselection procedure has a large effect, as can be seen in the performance of LCD-BST. This method shows a larger recall at the same level of FPR for each of the settings, approaching the ICP result in all cases. When we compare LCD-BST-MV to LCD-BST, it is seen that the choice of using either the partial correlation test or the more complex mean-variance test has almost no effect on the evaluation with respect to the top scoring pairs.

Table 1: Computation Times (CPU hours)

L_2 -BOOSTING	ICP	LCD	LCD-MV	LCD-BST	LCD-BST-MV
118	585	17	1936	133	172

Computation times are shown in Tab. 1 for each method, where we report the total time of computing all pairwise predictions over all 100 subsamples.⁵ The mean-variance test is two orders of magnitude slower in LCD-MV than simply running LCD with partial correlations, while having little to no effect on outcomes (Fig. 4). Preselecting results with the L_2 -boosting leads to a sparse enough set of possible parents such that a speedup is seen for the LCD-BST-MV estimator, in addition to increased precision. Applying the L_2 -boosting preselection to the simplest LCD implementation, LCD, which uses the fast partial correlations test, results in a much slower and equally performing LCD-BST estimator.

We also find that ICP is several times slower than LCD-BST-MV, the estimator that uses the same preselection and independence test as ICP. Notably, ICP is even less efficient when compared to LCD-BST, while both LCD-BST and LCD-BST-MV are very similar in performance to ICP.

5 Conclusion

Inspired by features of the ICP estimator, we implemented several different practical estimators of LCD, a simple constraint-based causal discovery method. We have shown that LCD predictions, computed on top of a L_2 -boosting procedure, can successfully predict the effects of unseen gene knock-outs in large-scale expression data. The estimator closely approximates the empirical performance of the state-of-the-art ICP, while it is algorithmically simpler and computationally more efficient. We also found that the predicted causal effects from LCD in this setting are robust under the choice of the independence test that is used. Surprisingly, a large part of the good performance is already explained by the L_2 -boosting preprocessing that these algorithms apply before causal considerations come into play.

⁵The CPUs used were comparable, where each subsample was randomly computed on either an Intel Xeon E5-2680, Intel Xeon E5-2680 or Intel Xeon Gold-5118 processor.

As we have seen, statistical aspects of causal discovery methods have a large impact on empirical performance. Nonetheless, they are largely underexplored for many practical algorithms. This leaves open the possibility for future work.

Acknowledgment

PV and JMM are supported by NWO, the Netherlands Organization for Scientific Research (VIDI grant 639.072.410).

References

- Stephan Bongers, Jonas Peters, Bernhard Schölkopf, and Joris M Mooij. Theoretical aspects of cyclic structural causal models. *arXiv preprint arXiv:1611.06221*, 2016.
- P. Bühlmann and S. van de Geer. *Statistics for High-Dimensional Data: Methods, Theory and Applications*. Springer, 2011.
- Peter Bühlmann and Bin Yu. Boosting with the l_2 loss: regression and classification. *Journal of the American Statistical Association*, 98(462):324–339, 2003.
- Lin S Chen, Frank Emmert-Streib, and John D Storey. Harnessing naturally randomized transcription to infer regulatory relationships among genes. *Genome biology*, 8(10):R219, 2007.
- G.F. Cooper. A simple constraint-based algorithm for efficiently mining observational databases for causal relationships. *Data Mining and Knowledge Discovery*, 1(2):203–224, 1997.
- Patrick Forré and Joris M Mooij. Markov properties for graphical models with cycles and latent variables. *arXiv preprint arXiv:1710.08775*, 2017.
- P. Kemmeren, K. Sameith, L.A. van de Pasch, J.J. Benschop, T.L. Lenstra, T. Margaritis, E. O’Duibhir, E. Apweiler, S. van Wageningen, C.W. Ko, S. van Heesch, M.M. Kashani, G. Ampatziadis-Michailidis, M.O. Brok, N.A. Brabers, A.J. Miles, D. Bouwmeester, S.R. van Hooff, H. van Bakel, E. Sluifers, L.V. Bakker, B. Snel, P. Lijnzaad, D. van Leenen, M.J. Groot Koerkamp, and F.C. Holstege. Large-scale genetic perturbations reveal regulatory networks and an abundance of gene-specific repressors. *Cell*, 157:740–752, 2014.
- N. Meinshausen and P. Bühlmann. Stability Selection (with discussion). *Journal of the Royal Statistical Society Series B*, 72:417–473, 2010.
- N. Meinshausen, A. Hauser, J.M. Mooij, J. Peters, P. Versteeg, and P. Bühlmann. Methods for causal inference from gene perturbation experiments and validation. *Proceedings of the National Academy of Sciences*, 113(27):7361–7368, 2016.
- J.M. Mooij and J. Cremers. An empirical study of one of the simplest causal prediction algorithms. pages 30–39.
- Joris M. Mooij, Sara Magliacane, and Tom Claassen. Joint Causal Inference from Multiple Contexts. *arXiv e-prints*, art. arXiv:1611.10351, Nov 2016.
- Judea Pearl. *Causality*. Cambridge university press, 2009.
- J. Peters, P. Bühlmann, and N. Meinshausen. Causal inference by using invariant prediction: identification and confidence intervals. *Journal of the Royal Statistical Society: Series B (Statistical Methodology)*, 78(5):947–1012, 2016.
- J. Peters, D. Janzing, and B. Schölkopf. *Elements of Causal Inference - Foundations and Learning Algorithms*. Adaptive Computation and Machine Learning Series. The MIT Press, Cambridge, MA, USA, 2017.
- Robert E Schapire, Yoav Freund, Peter Bartlett, Wee Sun Lee, et al. Boosting the margin: A new explanation for the effectiveness of voting methods. *The annals of statistics*, 26(5):1651–1686, 1998.

- P. Spirtes, C. Glymour, and R. Scheines. *Causation, Prediction, and Search*. MIT Press, second edition, 2000.
- R. Tibshirani. Regression shrinkage and selection via the Lasso. *Journal of the Royal Statistical Society, Series B*, 58:267–288, 1996.
- Sofia Triantafillou, Vincenzo Lagani, Christina Heinze-Deml, Angelika Schmidt, Jesper Tegner, and Ioannis Tsamardinos. Predicting causal relationships from biological data: Applying automated causal discovery on mass cytometry data of human immune cells. *Scientific reports*, 7(1):12724, 2017.